ChemComm

ROYAL SOCIETY OF CHEMISTRY

COMMUNICATION

View Article Online
View Journal | View Issue

Cite this: *Chem. Commun.*, 2020, **56**, 9998

Received 8th June 2020,
Accepted 20th July 2020

DOI: 10.1039/d0cc04011h

rsc.li/chemcomm

Natural-abundance ^{17}O NMR spectroscopy of magnetically aligned lipid nanodiscs†

Thirupathi Ravula, Bikash R. Sahoo, Xiaofeng Dai and Ayyalusamy Ramamoorthy *

Natural-abundance ^{17}O NMR experiments are used to investigate the hydrated water in magnetically aligned synthetic polymer based lipid-nanodiscs. Residual quadrupole couplings (RQCs) measured from the observed five ^{17}O (central and satellite) transitions, and molecular dynamics simulations, are used to probe the ordering of water molecules across the lipid bilayer.

Water is central to all life, and crucial for the structure and function of all biological systems. Study of hydration dynamics can provide valuable insights into the role of water in the function of such biological systems including proteins, RNA and biomaterials.[1,2] For example, water significantly influences the structure, dynamics and variety of functional properties of the cell membrane.[2,3] However, there are numerous challenges for high-resolution probing of the structure and dynamics of water molecules in a membrane environment. Herein, we demonstrate the use of natural-abundance ^{17}O NMR spectroscopy to investigate the interaction of water molecules with lipid-nanodiscs.

While the very low-abundance (~0.037%) and small gyromagnetic ratio (~1/7th of ^{1}H) render ^{17}O NMR insensitive, magic angle spinning (MAS) studies on solids well utilized the large chemical shift span and quadrupolar interaction of ^{17}O.[4,5] ^{17}O quadrupole central transition has also been used to study chemical and biological macromolecules in solution as reported in the literature.[4,6–9] In this study, polymer nanodiscs are used as membrane mimetics to investigate the interaction of water with lipid bilayers using natural-abundance ^{17}O NMR spectroscopy. Polymer nanodiscs consist of a planar lipid bilayer encased by a polymer belt (Fig. 1A).[10,11] Lipid nanodisc technology is increasingly used for structure and functional studies of membrane proteins.[12,13] While isotropic nanodiscs are used in solution NMR studies, the magnetic-alignment properties of polymer nanodiscs (diameter >20 nm) have been shown to be unique in enabling the application of solid-state NMR experiments to study lipids and membrane proteins, and to measure RDCs (residual dipolar couplings) using solution NMR studies.[14–17] Natural-abundance ^{17}O NMR spectra of magnetically-aligned and flipped nanodiscs are remarkable in showing all five transitions for the spin 5/2 system, and the exciting feasibility of using the experimentally measured residual quadrupolar couplings (RQCs) to determine the orientation of the water molecules in the lipid bilayer. A combination of NMR and molecular dynamic simulation presented here reveals the molecular level ordering of water molecules across the lipid bilayer.

Nanodiscs were prepared by the addition of a synthetic polymer (styrene maleimide quaternary ammonium (SMA-QA); synthesis, purification and characterization can be found elsewhere[15]) and DMPC (1,2-dimyristoyl-*sn-glycero*-3-phosphocholine) lipids as described in the ESI,† and characterized using biophysical experiments as reported previously.[18] The polymer nanodiscs prepared in various concentrations and their ability to magnetically align in the presence of an external magnetic field were confirmed using ^{31}P NMR as reported previously.[16,18] In addition, TEM images were used to confirm the approximate size and shape of the nanodiscs (see Fig. 1B). ^{17}O NMR experiments on varying concentrations of SMA-QA-DMPC nanodiscs were performed at 310 K, and the acquired spectra are shown in Fig. 1C. At a low lipid concentration (10% w/v), a single peak corresponding to the isotropic chemical shift frequency of water was observed. The scalar coupling between ^{17}O and ^{1}H resulting in a triplet for isotropic water is not observed for water in the nanodisc sample as the observed line is broader (line width is ~167 Hz) than the scalar coupling (~78 Hz). When the lipid concentration was increased to 20% w/v, the line-width of the observed ^{17}O peak increased to ~606 Hz and also showed a triplet pattern. Further increase in the concentration of the nanodiscs to 30% w/v showed a well-resolved pentet pattern as shown in Fig. 1C. Motion of water molecules in the nanodisc sample averaged the ^{17}O quadrupole coupling to a smaller value (called

Biophysics and Department of Chemistry, University of Michigan, Ann Arbor, MI 48109-1055, USA. E-mail: ramamoor@umich.edu

† Electronic supplementary information (ESI) available. See DOI: 10.1039/d0cc04011h

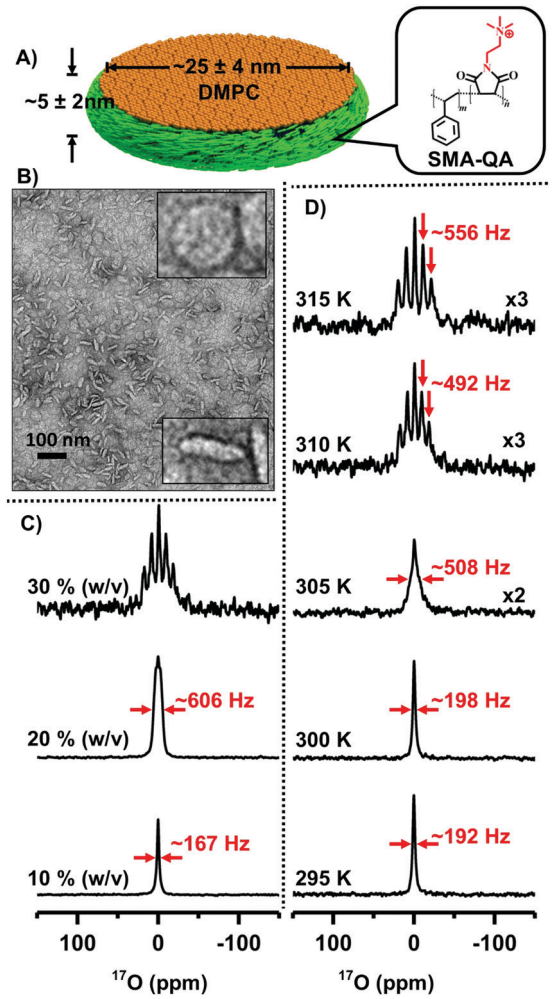

Fig. 1 Natural-abundance ^{17}O NMR spectra of polymer nanodiscs. (A) Schematic representation of SMA-QA polymer based lipid-nanodiscs. (B) TEM image of SMA-QA : DMPC (0.5 : 1 w/w) nanodiscs. ^{17}O NMR spectra of water from SMA-QA : DMPC (0.5 : 1 w/w) nanodiscs (~25 nm diameter) for varying lipid concentration at 310 K (C) and at the indicated temperatures for 30% w/v lipid concentration (D). All other details on the sample preparation, characterization, and experimental conditions are given in the ESI.†

RQCs) such that all five (one central and four satellite) transitions were observed in the form of a pentet pattern. The RQC values are obtained by measuring the frequency difference between any of the two adjacent peaks from the pentet signal; a value of ~492 Hz is measured for 30% w/v nanodiscs. These results suggest that water in magnetically-aligned nanodiscs is partially aligned.

To measure the effect of temperature on the alignment of water molecules in nanodiscs, ^{17}O spectra were recorded as a function of temperature (Fig. 1D). As demonstrated using ^{31}P and ^{14}N NMR experiments, the nanodiscs are isotropic at temperatures below the main gel to liquid crystalline phase transition temperature of DMPC (T_m ~ 24 °C) and magnetically align above T_m.[16] It is remarkable that ^{17}O RQC values observed for water in nanodiscs reveal the magnetic-alignment of the nanodiscs as shown in Fig. 1D. ^{17}O spectra show an isotropic peak below T_m at 295 and 300 K with line-widths <200 Hz, while increasing temperature resulted in line-broadening near T_m (see the spectrum at 305 with line-width ~508 Hz) exhibiting a poorly resolved splitting from the motionally-averaged RQC from nanodiscs. On the other hand, a multiplet pattern is observed above T_m as shown for the spectrum at 310 K with an RQC of ~492 Hz. Further increase in the temperature to 315 K increased the observed quadrupolar coupling to ~556 Hz. These observations clearly demonstrate the use of ^{17}O NMR spectra to probe the water molecule ordering using magnetic-alignment of the nanodiscs. To gain further insights into the dynamics of water, we measured the longitudinal relaxation (T_1) times for all five ^{17}O peaks observed (Fig. 3). The T_1 values for water molecules in the nanodiscs are in the range of 4 ms, and much smaller than that for bulk water (~9 ms, Fig. S2, ESI†), suggesting the restricted motion of water molecules in nanodiscs under these conditions.

Since the observed RQC depends on the order parameter as well as on the orientation of bilayer-associated water molecules, a single ^{17}O RQC value obtained from aligned nanodiscs is not sufficient to completely describe the alignment of water molecules. A complete description of the alignment of water molecules requires RDC values measured under different alignment conditions. To measure the RQCs of ^{17}O under different alignment conditions, we used a paramagnetic salt, $YbCl_3$, to flip the orientation of magnetically-aligned nanodiscs as described in our previous study.[16] ^{31}P and ^{14}N NMR experiments were used to confirm the flipping of the aligned nanodiscs upon the addition of $YbCl_3$. The effect of different paramagnetic salts on the NMR spectra and relaxation parameters of the nanodiscs is reported in our previous study.[19] The observed chemical shift for ^{31}P (from −13.6 ± 0.5 ppm to ~22.7 ± 3.7 ppm upon flipping) and doubling of ^{14}N RQC (from ~8.9 ± 0.6 kHz to ~16.8 ± 0.7 kHz upon flipping) confirmed the 90° flipping of the nanodiscs to result in a parallel orientation of the lipid bilayer normal to the external magnetic field direction (Fig. 2). ^{17}O NMR spectra of water in the flipped nanodiscs showed a significant increase in the RQC value: from 492 Hz to 690 Hz upon flipping as shown in Fig. 2(A and B). ^{17}O NMR spectra of varying concentrations of flipped and unflipped nanodiscs are shown in Fig. S1 (ESI†) along with deconvoluted spectra illustrating the multiplet pattern and RQC values. While it is remarkable that the motionally averaged water RQCs are sensitive to the alignment of the nanodiscs, the 90° flipping of aligned nanodiscs did not follow $(3\cos^2\phi - 1)$ for the observed ^{17}O RQCs unlike the ^{31}P and ^{14}N spectra, where ϕ is the angle between the bilayer normal and the magnetic field axis. The observed changes for ^{31}P and ^{14}N are because the axis of motional averaging for lipids (collinear with the bilayer normal) is oriented perpendicular (Fig. 2E) and parallel (2J) to the magnetic field axis. On the other hand, the bilayer-associated water molecules are in exchange with the free water molecules and are randomly oriented with respect to the bilayer normal. Even though the bilayer-associated water molecules prefer to orient with their symmetry (or the bisector) axes collinear with the bilayer normal as reported for zwitterionic lipids,[20] the

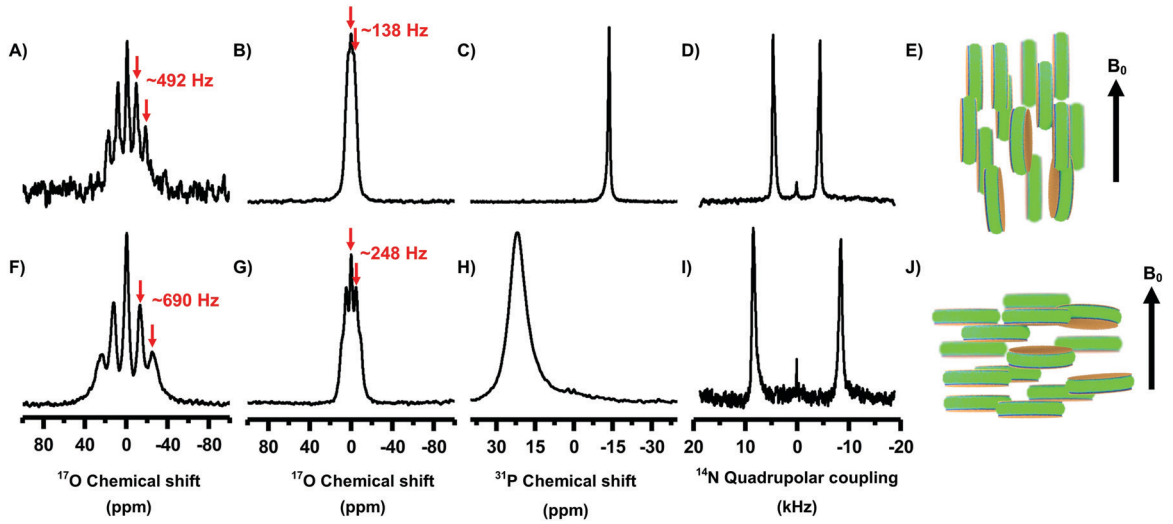

Fig. 2 NMR spectra of magnetically-aligned and flipped nanodiscs. ^{17}O (A, B, F and G), ^{31}P (C and H) and ^{14}N (D and I) NMR spectra of magnetically-aligned SMA-QA : DMPC nanodiscs obtained at 310 K with the lipid-bilayer-normal perpendicular (top row, as illustrated in E) and parallel (bottom row, as illustrated in J) to the external magnetic field direction. A 2 mM $YbCl_3$ was used to flip the nanodiscs (bottom row). All spectra were acquired from 20% w/v lipid concentration, except that 30% w/v was used for A and F. Deconvolution of the ^{17}O pentet spectra of aligned and flipped nanodiscs (20% and 30% w/v) are shown in Fig. S1 (ESI†).

observed RQC values indicate that the motional averaging of the ^{17}O quadrupolar coupling is different in flipped and unflipped nanodiscs, which is more pronounced when the concentration decreases (Fig. S1, ESI†). Therefore, ^{17}O RQCs can be useful to probe the molecular events at the membrane–water interface.

To explore the origins of the increase in the quadrupolar coupling upon 90° flipping of the nanodiscs, we used MD simulation using DMPC and water as a system (Fig. 4A); additional details are given in the ESI.† The main axis of the ^{17}O quadrupolar coupling tensor is perpendicular to the molecular plane of water as reported elsewhere.[21] To obtain the relative orientations and average RQCs for the quadrupole coupling tensor across the lipid bilayer, $\cos\theta$ values were calculated. MD simulations show a gradual decrease in water density across the bilayer (*i.e.* along the *z*-axis) and become zero in the hydrophobic core of the bilayer (Fig. 4B). With the DMPC bilayer placed along the *xy*-plane, space and time-averaged $\langle 3\cos^2\theta - 1\rangle$ values were calculated (Fig. 4C). The resulting $\langle 3\cos^2\theta - 1\rangle$ values are positive along the *z*-axis and negative along the *x* and *y* axes. The larger $\langle 3\cos^2\theta - 1\rangle$ magnitude along the *z*-axis suggests that the motional averaging along the *x* and *y* axes more effectively reduces the RQCs than that along the *z*-axis. These results are in agreement with the observed larger RQC values for the flipped-nanodiscs, which have the bilayer-normal (*i.e.* the *z*-axis in Fig. 4) along the magnetic field axis (Fig. 2J). Thus, the measured ^{17}O RQCs can be used to probe the ordering and dynamics of water molecules associated with a lipid bilayer.

In conclusion, we have demonstrated that natural-abundance ^{17}O NMR is a useful technique to study the magnetic-alignment of lipid-nanodiscs and also to probe membrane water interactions. At optimum hydration levels under the magnetic-alignment of nanodiscs, all five transitions of ^{17}O nuclei are observed. The measured RQCs are explained based on the orientation preference

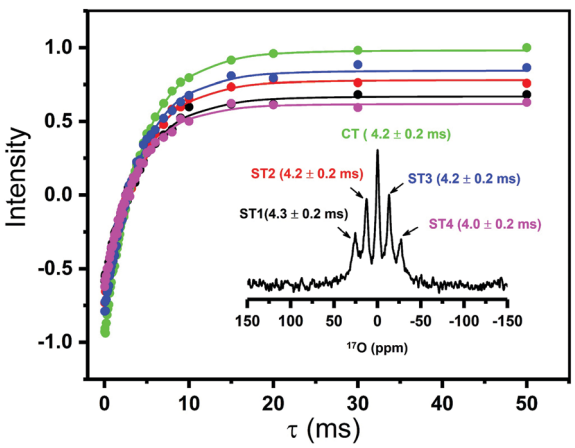

Fig. 3 T_1 relaxation of ^{17}O NMR transitions. ^{17}O spin–lattice (T_1) relaxation for the central (CT) and satellite transitions (ST1, ST2, ST3, ST4) measured from SMA-QA–DMPC (30% w/v) nanodiscs containing a 2 mM $YbCl_3$. ^{17}O NMR spectrum labelled with the transitions and the measured T_1 values (inset). T_1 values were obtained from the best-fitting of the inversion-recovery intensities (data points). See Fig. S2 (ESI†) for ^{17}O T_1 experimental data obtained from isotropic water, and Fig. S3 (ESI†) for ^{17}O inversion recovery NMR spectra of water present in nanodiscs.

of bilayer-associated water molecules. Overall, the reported results clearly indicate the molecular level ordering of water across the bilayer, and a combination of ^{17}O NMR and MD simulation can be used to further probe water–membrane interactions. The reported ^{17}O NMR experiments can also be used to investigate other aligned samples such as other types of nanodiscs,[22,23] bicelles,[24–28] and other alignment media used in NMR studies.[29] We also expect the reported approach and results to be useful in the investigation of the role of ordered water in many biological processes including protein folding,

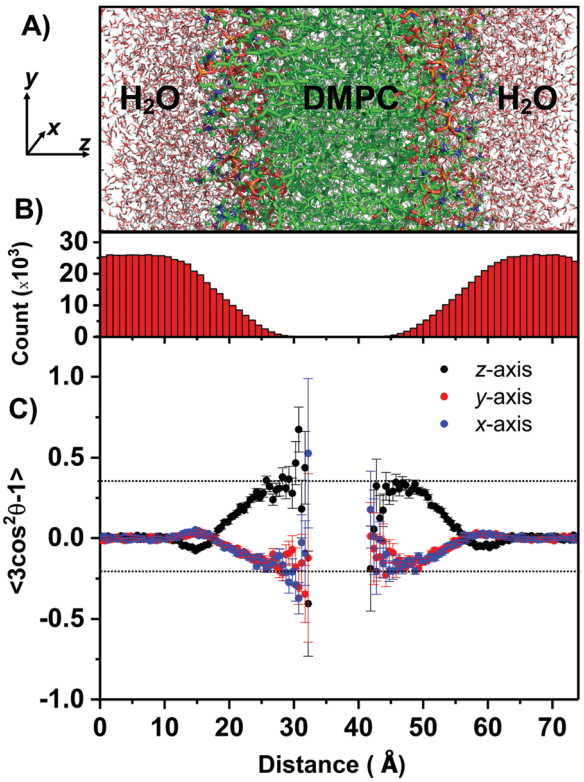

Fig. 4 (A) Selected region of the DMPC:water system (consisting of 256 DMPC and 10 153 water molecules) used in molecular dynamic simulations; additional details can be found in the ESI† (Fig. S4 and S5). (*x*, *y*, *z*) coordinates are shown with the *z*-axis parallel to the lipid bilayer normal. (B) Total number of water molecules present in the *xy* plane plotted along the *z*-coordinate (*i.e.* lipid-bilayer normal) throughout the simulation time. (C) Space and time-averaged $\langle 3\cos^2\theta - 1\rangle$ as a function of the *z*-coordinate; where θ is the angle between the normal to the water plane (*i.e.* the main principal axis of ^{17}O quadrupole coupling tensor) and the *x* (blue), *y* (red), and *z* (black) axes. Space averaging was carried out for all water molecules present in the *xy* plane for each point along the *z*-axis. The error bar represents the standard deviation from the average value. The large error bars are due to the presence of less water molecules in the core of the bilayer. See the ESI† for additional details on the simulations used in this study.

misfolding, amyloid aggregation, and biomineralization processes.[30–32] The use of dynamic nuclear polarization experiments[33,34] to enhance ^{17}O NMR sensitivity for studies on aligned samples[35,36] would be exciting.

This study was supported by NIH (GM084018 to AR). We thank Dr Ganapathy, a visiting researcher in the Ramamoorthy lab, for help with the initial ^{17}O NMR experiments.

Conflicts of interest

There are no conflicts to declare.

Notes and references

1 P. Ball, *Chem. Rev.*, 2008, **108**, 74–108.
2 M. Chaplin, *Nat. Rev. Mol. Cell Biol.*, 2006, **7**, 861–866.
3 E. A. Disalvo, F. Lairion, F. Martini, E. Tymczyszyn, M. Frias, H. Almaleck and G. J. Gordillo, *Biochim. Biophys. Acta*, 2008, **1778**, 2655–2670.
4 F. Castiglione, A. Mele and G. Raos, in *Annual Reports on NMR Spectroscopy*, ed. G. A. Webb, Academic Press, 2015, vol. 85, pp. 143–193.
5 M. T. McMahon, A. C. deDios, N. Godbout, R. Salzmann, D. D. Laws, H. Le, R. H. Havlin and E. Oldfield, *J. Am. Chem. Soc.*, 1998, **120**, 4784–4797.
6 E. G. Keeler, V. K. Michaelis, C. B. Wilson, I. Hung, X. Wang, Z. Gan and R. G. Griffin, *J. Phys. Chem. B*, 2019, **123**, 3061–3067.
7 G. Wu, *Prog. Nucl. Magn. Reson. Spectrosc.*, 2019, **114–115**, 135–191.
8 K. Kouril, B. Meier, S. Alom, R. J. Whitby and M. H. Levitt, *Faraday Discuss.*, 2018, **212**, 517–532.
9 N. Rezaei-Ghaleh, F. Munari, S. Becker, M. Assfalg and C. Griesinger, *Chem. Commun.*, 2019, **55**, 12404–12407.
10 T. Ravula, N. Z. Hardin and A. Ramamoorthy, *Chem. Phys. Lipids*, 2019, **219**, 45–49.
11 M. C. Orwick, P. J. Judge, J. Procek, L. Lindholm, A. Graziadei, A. Engel, G. Grobner and A. Watts, *Angew. Chem., Int. Ed.*, 2012, **51**, 4653–4657.
12 J. M. Dorr, M. C. Koorengevel, M. Schafer, A. V. Prokofyev, S. Scheidelaar, E. A. van der Cruijsen, T. R. Dafforn, M. Baldus and J. A. Killian, *Proc. Natl. Acad. Sci. U. S. A.*, 2014, **111**, 18607–18612.
13 S. C. Lee, T. J. Knowles, V. L. Postis, M. Jamshad, R. A. Parslow, Y. P. Lin, A. Goldman, P. Sridhar, M. Overduin, S. P. Muench and T. R. Dafforn, *Nat. Protoc.*, 2016, **11**, 1149–1162.
14 T. Ravula and A. Ramamoorthy, *Angew. Chem., Int. Ed.*, 2019, **58**, 14925–14928.
15 T. Ravula, N. Z. Hardin, S. K. Ramadugu, S. J. Cox and A. Ramamoorthy, *Angew. Chem., Int. Ed.*, 2018, **57**, 1342–1345.
16 T. Ravula, J. Kim, D. K. Lee and A. Ramamoorthy, *Langmuir*, 2020, **36**, 1258–1265.
17 J. Radoicic, S. H. Park and S. J. Opella, *Biophys. J.*, 2018, **115**, 22–25.
18 T. Ravula, S. K. Ramadugu, G. Di Mauro and A. Ramamoorthy, *Angew. Chem., Int. Ed.*, 2017, **56**, 11466–11470.
19 G. M. Di Mauro, N. Z. Hardin and A. Ramamoorthy, *Biochim. Biophys. Acta, Biomembr.*, 2020, **1862**, 183332.
20 J. X. Cheng, S. Pautot, D. A. Weitz and X. S. Xie, *Proc. Natl. Acad. Sci. U. S. A.*, 2003, **100**, 9826–9830.
21 O. V. Yazyev and L. Helm, *J. Chem. Phys.*, 2006, **125**, 054503.
22 M. L. Nasr, D. Baptista, M. Strauss, Z. J. Sun, S. Grigoriu, S. Huser, A. Pluckthun, F. Hagn, T. Walz, J. M. Hogle and G. Wagner, *Nat. Methods*, 2017, **14**, 49–52.
23 I. G. Denisov and S. G. Sligar, *Chem. Rev.*, 2017, **117**, 4669–4713.
24 O. F. Lange, N. A. Lakomek, C. Fares, G. F. Schroder, K. F. Walter, S. Becker, J. Meiler, H. Grubmuller, C. Griesinger and B. L. de Groot, *Science*, 2008, **320**, 1471–1475.
25 C. R. Sanders, B. J. Hare, K. P. Howard and J. H. Prestegard, *Prog. Nucl. Magn. Reson. Spectrosc.*, 1994, **26**, 421–444.
26 N. Tjandra and A. Bax, *Science*, 1997, **278**, 1111–1114.
27 J. H. Prestegard, C. M. Bougault and A. I. Kishore, *Chem. Rev.*, 2004, **104**, 3519–3540.
28 A. C. Stelzer, A. T. Frank, M. H. Bailor, I. Andricioaei and H. M. Al-Hashimi, *Methods*, 2009, **49**, 167–173.
29 K. Chen and N. Tjandra, *NMR of Proteins and Small Biomolecules*, ed. G. Zhu, Springer Berlin Heidelberg, Berlin, Heidelberg, 2012, pp. 47–67, DOI: 10.1007/128_2011_215.
30 T. Wang, H. Jo, W. F. DeGrado and M. Hong, *J. Am. Chem. Soc.*, 2017, **139**, 6242–6252.
31 D. Thirumalai, G. Reddy and J. E. Straub, *Acc. Chem. Res.*, 2012, **45**, 83–92.
32 D. C. Rodriguez Camargo, K. J. Korshavn, A. Jussupow, K. Raltchev, D. Goricanec, M. Fleisch, R. Sarkar, K. Xue, M. Aichler, G. Mettenleiter, A. K. Walch, C. Camilloni, F. Hagn, B. Reif and A. Ramamoorthy, *eLife*, 2017, **6**, e31226.
33 Y. Su, L. Andreas and R. G. Griffin, *Annu. Rev. Biochem.*, 2015, **84**, 465–497.
34 S. L. Carnahan, B. J. Lampkin, P. Naik, M. P. Hanrahan, I. I. Slowing, B. VanVeller, G. Wu and A. J. Rossini, *J. Am. Chem. Soc.*, 2019, **141**, 441–450.
35 E. Salnikov, M. Rosay, S. Pawsey, O. Ouari, P. Tordo and B. Bechinger, *J. Am. Chem. Soc.*, 2010, **132**, 5940–5941.
36 O. Jakdetchai, V. Denysenkov, J. Becker-Baldus, B. Dutagaci, T. F. Prisner and C. Glaubitz, *J. Am. Chem. Soc.*, 2014, **136**, 15533–15536.